Catalysis Letters Vol. 99, Nos. 3–4, February 2005 (© 2005)
DOI: 10.1007/s10562-005-2131-7

Mössbauer spectra and catalytic behavior of perovskite-like $SrFe_{0.7}Al_{0.3}O_{3-\delta}$

V.V. Kharton,[1,*] J.C. Waerenborgh,[2] D.P. Rojas,[2] A.A. Yaremchenko,[1] A.A. Valente,[3] A.L. Shaula,[1] M.V. Patrakeev,[1,4] F.M.B. Marques[1] and J. Rocha[3]

[1]*Department of Ceramics and Glass Engineering, CICECO, University of Aveiro, 3810-193 Aveiro, Portugal*
[2]*Chemistry Department, ITN/CFMC-UL, Estrada Nacional 10, P-2686-953 Sacavèm, Portugal*
[3]*Department of Chemistry, CICECO, University of Aveiro, 3810-193 Aveiro, Portugal*
[4]*Institute of Solid State Chemistry, Ural Division of RAS, 91 Pervomaiskaya Str., Ekaterinburg 620219, Russia*

Received ■; accepted 15 October 2004

Mixed-conducting $SrFe_{0.7}Al_{0.3}O_{3-\delta}$ (SFA) exhibits substantial catalytic activity towards partial oxidation of methane and can thus be considered as a component of monolithic ceramic reactors for synthesis gas generation, where the dense membrane and porous catalyst at the permeate-side surface are made of similar compositions. Surface modification of SFA powder and membranes with Pt has no essential effect on the performance of a model reactor, suggesting that the catalytic behavior of SFA is mainly determined by the surface states of iron and oxygen ions in the catalyst. The Mössbauer spectroscopy shows that reduction of $SrFe_{0.7}Al_{0.3}O_{3-\delta}$, having cubic perovskite lattice in air, leads to the co-existence of perovskite- and brownmillerite-like domains, whilst the concentrations of metallic Fe and even Fe^{2+} under typical operation conditions are lower than the detection limits. The amount of vacancy-ordered phase increases with decreasing oxygen content, the estimations of which were confirmed by coulometric titration data. The catalytic activity of ferrite-based materials may thus be associated with lattice instability characteristic of morphotropic phase transformations.

KEY WORDS: methane oxidation; Mössbauer spectroscopy; strontium ferrite; membrane reactor; synthesis gas; oxygen nonstoichiometry; mixed conductor.

1. Introduction

Synthesis gas (syngas), a mixture of CO and H_2, is an important feedstock for commercial Fischer–Tropsch and methanol synthesis [1,2]. To date, large-scale industrial route for syngas production comprises steam reforming of methane, which is, however, a capital- and energy-intensive process and also gives H_2/CO ratio higher than optimum. Possible alternative routes include the catalytic partial oxidation of methane (POM) and the use of dense ceramic membranes with mixed oxygen-ionic and electronic conductivity [1–5]. Although the former is a mildly exothermic process yielding an ideal H_2/CO ratio of 2, the industrial-scale application of POM is confined due to the high costs of cryogenic oxygen plants [1–4].

Contrary to conventional technologies, the membrane reactors make it possible to combine oxygen separation from air, POM and reforming, thus enabling to significantly reduce the capital investments into gas-to-liquid industry [4,5]. At the same time, the development of commercially feasible membrane technologies for syngas generation is essentially limited due to materials science problems, particularly as a result of rigid requirements to physicochemical, thermomechanical and transport properties of mixed-conducting ceramics. One important aspect in these developments relates to the catalytic activity of membrane materials. Most promising mixed conductors are based on perovskite-related oxide phases containing transition metal cations [5]. As a rule, the transition metal oxides are active for complete oxidation rather than for the POM; a high activity with respect to the partial oxidation is typical for metal-oxide mixtures, where the steam and/or CO_2 reforming stage on the metal surface follows the reaction of total CH_4 oxidation on the oxide surface [1]. This makes it necessary to incorporate reforming catalysts in the membrane reactors. On the other hand, significant technological and economic advantages could be expected for the monolithic reactors where a thick-film membrane is applied onto porous ceramics, the latter simultaneously acting as a catalyst support, providing necessary mechanical strength and also enhancing the specific surface area of the membrane [5,6]. Due to high operation temperatures, 970–1170 K, using of similar compositions for the membrane and for the support is preferable in order to minimize long term degradation processes caused by cation interdiffusion. The choice of such compositions should obviously account their catalytic activity towards POM, with or without additional surface modification.

This work continues our studies [7–9] of mixed-conducting membranes for natural gas conversion and

*To whom correspondence should be addressed.
E-mail: kharton@cv.ua.pt

presents data on the behavior of perovskite-like $SrFe_{0.7}Al_{0.3}O_{3-\delta}$ (SFA), which can be considered as a possible parent material for the monolithic reactors due to an attractive combination of stability, oxygen transport and catalytic properties [9,10]. In particular, oxidation of CH_4 pulses on the surface of SFA powder results in selective formation of synthesis gas with a H_2/CO ratio close to 2, characteristic of the POM process [9]. Such a trend, rather exceptional for transition metal-containing oxides [1], was earlier observed for several perovskite-related ferrites at temperatures above 970 K [11–13]. One possible explanation based on the results of temperature-programmed reduction (TPR) and pulse experiments, ascribed the high selectivity towards POM to strongly bonded lattice oxygen having a low mobility [11–13]. In order to reveal if the steady-state oxidation of methane by oxygen permeating through dense oxide ceramics may occur via similar mechanisms, in this work SFA powder was tested in a model reactor comprising one disk-shaped membrane and a catalyst both made of the title composition. Special emphasis was also given to the evaluation of iron oxidation states, which may be responsible for the catalytic behavior of SFA, by the Mössbauer spectroscopy.

2. Experimental

The powder of SFA, was prepared via glycine–nitrate process (GNP), a self-combustion technique using glycine as a fuel and nitrates of metal components as oxidant [14]. In the course of GNP, glycine was added into an aqueous solution containing metal cations in stoichiometric proportion; the glycine/nitrate molar ratio was twice of the stoichiometric one, assuming the only gaseous products of reaction to be N_2, CO_2 and H_2O. The solution was dried and heated until auto-ignition; the obtained powder having foam-like structure was annealed at 1073 K in air in order to remove organic residuals. Gas-tight ceramics were pressed at 200–250 MPa and sintered in air at 1520–1600 K for 2 h. The density of ceramics was higher than 95% of theoretical. The powdered samples, used for X-ray diffraction (XRD) and Mössbauer spectroscopy studies, were obtained by grinding of dense ceramics and annealing at 1023 K for 3–5 h in various atmospheres. The samples equilibrated in air were either slowly cooled (1–2 K/min) down to room temperature or quenched in liquid nitrogen. Another series of the powdered samples were treated in flowing Ar and in a H_2–H_2O–N_2 mixture with subsequent fast cooling (10–12 K/min); the oxygen partial pressure in these atmospheres, measured by an electrochemical oxygen sensor, was 10^{-5} and 10^{-17} atm, respectively. The latter $p(O_2)$ value was selected as typical for non-equilibrium mixtures of CH_4 conversion products in the membrane reactors, where the mixed-conducting ceramics possess moderate oxygen permeability, close to that of SFA [8,9].

The XRD patterns were obtained at room temperature using a Rigaku D/MAX-B diffractometer (CuKα radiation, 2Θ = 20–80°, step 0.02°, 1 s/step). The Mössbauer spectra were collected at room temperature and at 15 K in transmission mode using a conventional constant-acceleration spectrometer and a 25 mCi ^{57}CO source in a Rh matrix; the low-temperature measurements were performed using a liquid-helium flow cryostat with a temperature stability of ± 0.5 K. The velocity scale was calibrated using an α-Fe foil. The absorbers were prepared by pressing the powdered samples (5 mg of natural Fe/cm^2) into perspex holders. The spectra were fitted to Lorentzian lines using a non-linear least-square method [15]; isomer shifts (IS, table 1) are given relative to metallic α-Fe at room temperature. For each quadruple doublet, the relative areas and widths of both peaks were kept equal during refinement. Distributions of quadruple splittings (QS) or magnetic splittings were fitted according to the histogram method [16]. The coulometric titration technique [17] was used to determine oxygen content as a function of oxygen partial pressure and temperature.

The studies of dry methane oxidation were performed using a model membrane reactor comprising one SFA disk hermetically sealed onto an yttria-stabilized zirconia (YSZ) tube (figure 1). The effective geometric area of the membrane surface exposed to methane flow was 63 ± 1 mm^2. In order to facilitate surface processes which may become oxygen flux-limiting in reducing atmospheres [8,9], highly porous layers of Pt or nanocrystalline SFA (table 2) were applied onto the permeate-side surface of SFA membranes; the nanocrystalline SFA powder was synthesized by the cellulose-precursor technique as described elsewhere [18]. The reactor was packed with a porous SFA catalyst prepared by grinding the GNP-synthesized ceramics sintered at 1273 K for 1 h (density of 38 ± 2%). After sieving, the fraction of particles with average size 0.5–1.5 mm was selected for packing. The specific surface area of the catalyst determined by the BET technique was 1.9 m^2/g. For the surface modification of this catalyst with platinum, the material was impregnated with an aqueous solution of H_2PtCl_4, dried and then annealed at 1373 K for I h. In the course of the experiments, dry CH_4 ($\geq$99.995% purity) diluted with He (50:50 vol.%) was supplied onto the permeate side of the membrane and the feed side was exposed to atmospheric air, such that oxygen permeated through the membrane and reacted with methane. The gas-flow composition and rate at the reactor inlet were fixed by Bronkhorst mass-flow controllers. The influent and effluent gas mixtures were analyzed using a Varian CP-3800 gas chromatograph equipped with thermal-conductivity and flame-ionization detectors coupled in series, a 250 μL six-port VICI gas-sampling valve and a semicapillary CarboPLOT P7 column. No impurities in

Table 1
Parameters estimated from the Mössbauer spectra of SFA

Measurement temperature	Pre-treatment	Phase	Iron state	IS (mm/s)	QS,ε (mm/s)	B_{hf}(T)	I (%)
295 K	Equilibrated at $p(O_2)$ = 0.21 atm, T = 1023 K	P	Fe^{3+}	0.29	1.07	85	
			Fe^{4+}	–0.03	0.33	15	
15 K	Equilibrated at $p(O_2)$=0.21 atm, T ≈ 295 K	P	Fe^{3+}	0.43	–0.02	47	75
			Fe^{4+}	0.11	0.17	22.3	25
	Equilibrated at $p(O_2)$ = 10^{-5} atm, T = 1023 K	P	Fe^{3+}	0.43	–0.02	46.7	36
			Fe^{4+}	0.12	0.10	21.0	11
		B	CN6-Fe^{3+}	0.47	–0.01	51.0	41
			CN4-Fe^{3+}	0.25	0.12	43.5	12
	Equilibrated at $p(O_2)$ = 10^{-17} atm, T = 1023 K	P	Fe^{3+}	0.44	–0.28	46.7	7
		B	CN6-Fe^{3+}	0.47	–0.01	53.1	80
			CN4-Fe^{3+}	0.22	0.16	45.6	13

Notes: P and B correspond to perovskite- and brownmillerite-like domains, respectively; CN6-Fe^{3+} and CN4-Fe^{3+} correspond to octahedrally and tetrahedrally coordinated Fe^{3+}; IS and QS are the isomer shift relative to metallic α-Fe at 295 K and the quadruple splitting of a quadruple doublet. ε and B_{hf} are the quadruple shift and the magnetic hyperfine field of a magnetic sextet respectively. For Fe^{3+} at 295 K IS and QS are average values estimated from QS distributions; for the 15 K spectra IS, and B_{hf} are average values estimated from B_{hf} distributions; I is the relative area; Estimated standard deviations are <2% for I <0.4 T for B_{hf} and <0.02 mm/s for the other parameters.

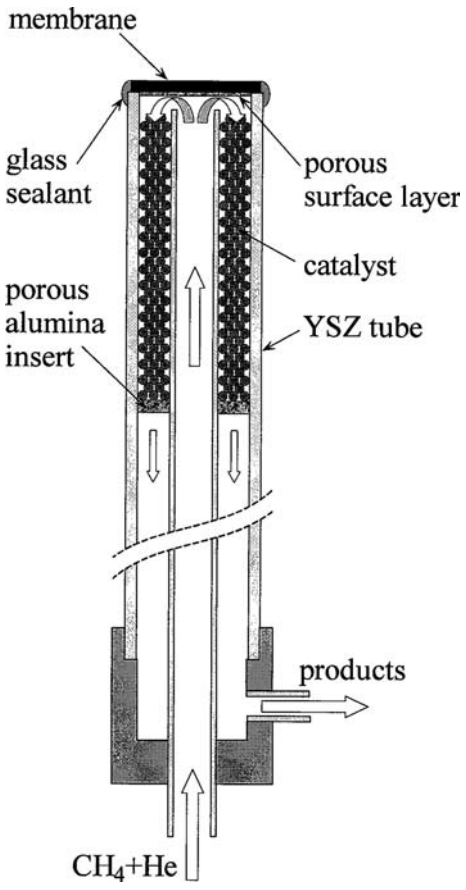

Figure 1. Schematic drawing of the membrane reactor for methane oxidation.

Table 2
Model reactors with SAF membranes for methane conversion

Reactor	Membrane thickness (mm)	Permeate-side layer			Catalyst
		Composition	Sheet density (mg/cm^2)	Sintering conditions	
1	0.95	Pt	7.6	1223 K, 0.3 h	None
2	0.95	Pt	7.7	1223 K, 0.3 h	SFA
3	0.60	SFA	4.7	1373 K, 1 h	Pt-modified SFA

the initial gas mixture, and also no leaking of air into the reactor, were detected. The reaction selectivity was calculated as the concentration ratio between a given product and the sum of all detected carbon-containing products, namely CO, CO_2, C_2H_2, C_2H_4 and C_2H_6.

3. Results and discussion

As for other mixed-conducting membranes [8,9], the oxidation of dry methane over the SFA membrane

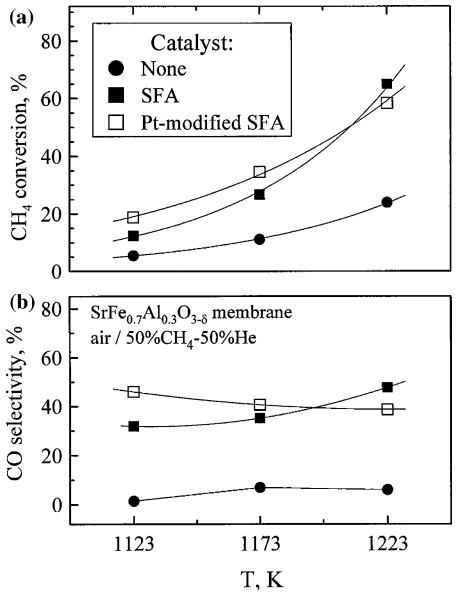

Figure 2. Methane conversion (a) and CO selectivity (b) in the membrane reactor with and without catalysts. The inlet flow rate of 50%CH_4–50%He mixture was 2.0 mL/min.

in a reactor without packing results in predominant total combustion (figure 2). Increasing temperature leads to a higher conversion due to increasing oxygen permeability; since no traces of O_2 were observed at the reactor outlet, the methane consumption is limited by the oxygen permeation fluxes. The yield of C2-hydrocarbons was found lower than 2% and decreased with temperature. The selectivity with respect to CO is also very low; at 1123–1223 K, the values of CO selectivity vary in the range 1–10%, increasing with temperature and CH_4 flow rate. The dominant formation of CO_2 suggests that oxidation reactions occur mainly on the surface of SFA ceramics, while the effect of porous Pt, well known as an active reforming catalyst [1–3], is rather minor. Furthermore, the observed behavior seems to indicate gas-phase transport limitations in combination with the total oxidation reaction promoted on the membrane surface by active oxygen species, formed due to partial discharge and recombination of O^{2-} ions transported through dense SFA ceramics; as a result, significant fraction of supplied CH_4 remains unreacted, being mixed with CO_2 and H_2O at the reactor outlet. The membrane material seems, hence, to play no essential role in the CH_4 oxidation mechanisms, except for the oxygen permeation rate, in agreement with data on other mixed conductors [8].

Packing of the membrane reactor with porous SFA catalyst, with or without surface modification, has a drastic effect on the methane conversion and CO selectivity (figure 2). The conversion at 1223 K achieves 60–65%, whilst the CO yield becomes similar to that of CO_2. Such an improvement is due to reforming of residual CH_4 with H_2O and CO_2 formed on the membrane surface; the composition of effluent gas mixtures became thus closer to thermodynamic equilibrium, as expected. At the same time, the equilibrium is not yet achieved. For instance, when the CH_4 conversion is lower than 96%, the thermodynamic calculations predict equilibrium CO yields higher than 90% at 1023 K (figure 3b). The values of CO selectivity, observed experimentally at this temperature, are about 46% and 32% for SFA catalyst with and without surface modification, respectively (figure 2). The selectivity to C2-hydrocarbons in the packed reactors decreased down to the limits of experimental uncertainty.

The behavior of Pt-modified SFA catalyst is, in general, similar to that of unmodified SFA, although the former provides a higher CO yield at 1123 K. This clearly indicates that the conversion rate and CO selectivity are both determined by the catalytic properties of SFA, in particular by the surface states of iron and oxygen ions. Note that, in order to avoid possible sintering of Pt particles on the surface of Pt-modified SFA in the course of catalytic tests, the experiments illustrated by figure 2 were performed with a stepwise decrease of the reactor operation temperature. If the temperature of catalyst pre-treatment, 1373 K, is insufficient, the maximum passivation rate could be expected at high temperatures such as 1223 K; no essential sintering should hence occur on subsequent cooling. Nevertheless, no degradation in the reactor performance

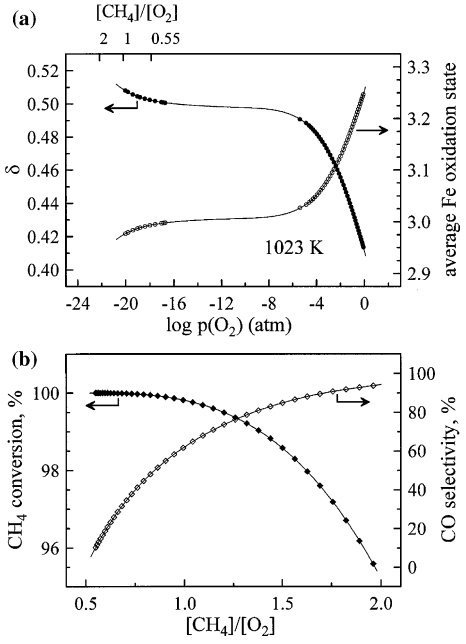

Figure 3. (a) Oxygen partial pressure dependencies of equilibrium oxygen non-stoichiometry and average iron oxidation state in SFA at 1023 K, determined by the coulometric titration technique and (b) the thermodynamically equilibrium values of CH_4 conversion and CO selectivity vs. CH_4:O_2 ratio in the initial mixture. The procedure used for thermodynamic calculations of CH_4 conversion was described in Ref. [19]. The upper axis in (a) shows equilibrium CH_4:O_2 ratio for the corresponding values of the oxygen partial pressure.

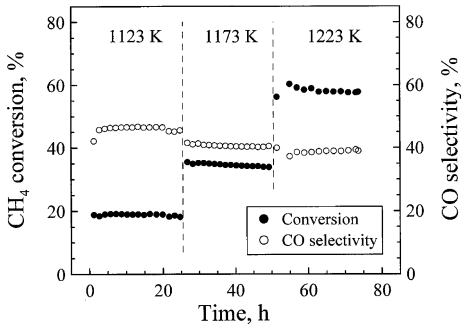

Figure 4. Time dependence of CH_4 conversion and CO selectivity in a reactor with SFA membrane and Pt-modified SFA catalyst. The inlet flow rate of 50% CH_4–50%He mixture was 2.0 mL/min.

with time was detected (figure 4), indicating that the decrease in CO selectivity over the Pt-modified SFA on increasing temperature (figure 2) cannot be attributed to Pt sintering.

The absence of time degradation of the reactor performance suggests also that there is no bulk reduction of the oxide phase into a mixture containing metallic iron. This conclusion was confirmed by XRD (figure 5). Furthermore, the XRD analysis did not reveal apparently the transition of perovskite into the vacancy-ordered brownmillerite phase, characteristic of strontium ferrite-based compounds ([20–22] and references cited). Most likely, these ordering processes cannot be distinguished by XRD due to low sensitivity of this method to oxygen sublattice. In order to evaluate exact phase composition and the states of iron in SFA lattice, the Mössbauer spectroscopy was used.

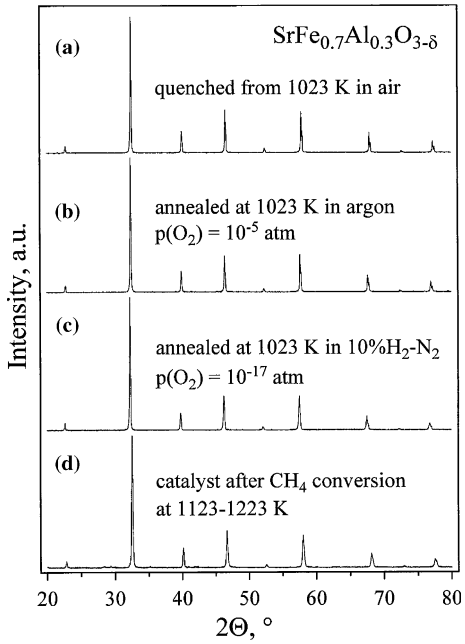

Figure 5. (a–c) XRD patterns of SFA after annealing in different atmospheres and (d) SFA catalyst after methane conversion tests at 1123–1223 K for 90 h.

The 295 K Mössbauer spectra of SFA equilibrated with atmospheric oxygen and then quenched from 1023 K or slowly cooled down to room temperature (figure 6a, b), are similar to those reported for $Sr(Fe,Ti)O_{3-\delta}$ perovskites [20–22]. In a first approximation, these spectra can be analyzed using only two doublets attributed to Fe^{4+} and Fe^{3+}. The Lorentzian peaks of the doublet with highest IS, the Fe^{3+} doublet are, however, broad and cannot reproduce correctly the shape of the spectrum envelope. The most obvious reason is that at least two different coordination numbers (CN) of iron, 5 and 6, are expected in the perovskite lattice of SFA. Disorder in the second and third coordination spheres due to the presence of oxygen vacancies and doping with aluminum should further increase the number of different contributions to the spectrum. These contributions are revealed by strong broadening of the doublet peaks since the corresponding differences in hyperfine parameters are not large enough to result in resolved contributions. Therefore, a distribution of Fe^{3+} quadruple doublets was refined. Additional improvement of the fitting was achieved when a correlation between IS and QS of this distribution was considered; the best results correspond to a decrease of 0.0375 mm/s in IS per 1 mm/s increase in QS, in

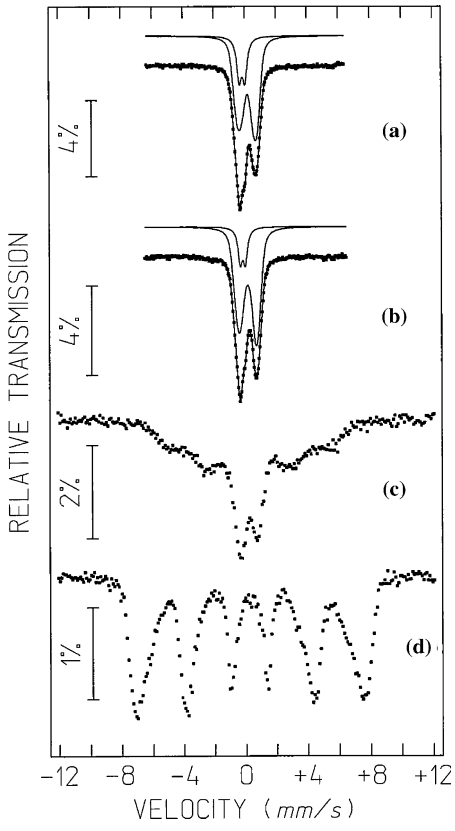

Figure 6. (a) Room-temperature Mössbauer spectra of SFA equilibrated at low temperatures in air; (b) annealed at 1023 K in air and then quenched; (c) annealed at 1023 K and $p(O_2) = 10^{-5}$ atm; and (d) annealed in a H_2–H_2O–N_2 flow at $p(O_2) = 10^{-17}$ atm.

agreement with data on the whole $SrFe_{1-x}Al_xO_{3-\delta}$ ($x = 0.1 - 0.5$) series which will be summarized in a separate publication. The estimated average IS, 0.29 mm/s, is consistent with the presence of 5- and 6-coordinated Fe^{3+} [22,23]. No significant improvement in the quality of the refinement was achieved replacing the Fe^{4+} quadruple doublet by a QS distribution.

In addition to a paramagnetic contribution observed for the samples equilibrated in air, the Mössbauer spectrum of SFA annealed at $p(O_2) = 10^{-5}$ atm shows the presence of a magnetic ordered phase (figure 6c). The absorption peaks are very broad, probably due to relaxation phenomena associated with the proximity of the magnetic ordering temperature. For reduced SFA annealed at $p(O_2) = 10^{-17}$ atm, the shape of the spectrum suggests all iron to be magnetically ordered (figure 6d). Due to peak broadening, no accurate information on the state of iron cations in the samples with low oxygen content may be obtained from the room-temperature Mössbauer data. Therefore, the spectra were collected at 15 K (figure 7), where the relaxation is slower and magnetic sextets should be observed. At this temperature, reduced SFA is close to magnetic saturation and the resolution is substantially better compared to the room-temperature data. For the sake of comparison, another spectrum of oxidized SFA equilibrated at room temperature in air was also obtained at 15 K (figure 7a). This spectrum was fitted considering two distributions of magnetic splittings

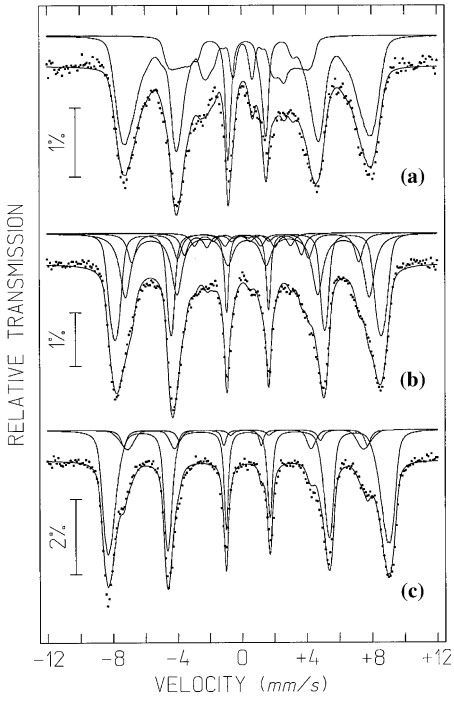

Figure 7. (a) Mössbauer spectra, collected at 15 K, for SFA equilibrated at low temperatures in air; (b) reduced at 1023 K and $p(O_2) = 10^{-5}$ atm; and (c) reduced at 1023 K and $p(O_2) = 10^{-17}$ atm. The spectra were collected at 15 K. Solid lines correspond to fitting results as described in the text and in table 1.

associated with Fe^{3+} and Fe^{4+} ions; the results were consistent with the room temperature data within the limits of experimental error. Table 1 summarizes the parameters estimated from the Mössbauer spectra.

Neither traces of metallic iron nor evidence of hyperfine splittings with low magnetic hyperfine field (B_{hf}), typical for Fe^{4+}, were observed for reduced SFA annealed at $p(O_2) = 10^{-17}$ atm. In fact, the corresponding spectrum (figure 7c) is well described using two distributions of magnetic splittings, with the average parameters consistent with those of 6- and 4-coordinated Fe^{3+} in a brownmillerite-type lattice [24,25]. The estimated relative areas I (table 1) seem to indicate that Al^{3+} prefers tetrahedral coordination, while Fe^{3+} exhibits a preference for octahedrally coordinated sites as observed in brownmillerite-type $Ca_2FeAlO_{5+\delta}$ [24,25]. A significant improvement in the fitting quality was further achieved when considering a third contribution, with the parameters typical for Fe^{3+} in a perovskite lattice such as those estimated for SFA equilibrated in air (table 1). The perovskite phase contains approximately 7% total iron amount in the SFA powder. Note, however, that these data cannot exclude a probability of metallic iron formation in SFA surface monolayer in the membrane reactors.

The sample annealed at $p(O_2) = 10^{-5}$ atm shows absorption peaks at the Doppler velocities, where the Fe^{4+} signal is observed for oxidized SFA (figure 7). Furthermore, the absorption between the outmost peaks due to tetrahedrally and octahedrally coordinated Fe^{3+} in the brownmillerite domains is also visible, suggesting the presence of magnetic sextets with intermediate IS and B_{hf} values, such as those observed for Fe^{3+} in perovskite. Therefore, as for reduced SFA, the perovskite- and brownmillerite-like phases co-exist at $p(O_2) = 10^{-5}$ atm. The spectrum shown in figure 7b was thus fitted with all contributions observed in the spectra of reduced and oxidized samples. Due to strong overlapping of all these contributions, the values of the hyperfine parameters were kept constant during refinement, with the intensities to be the only regression parameters and separate adjustment of the fixed hyperfine parameters.

The average oxidation states of iron cations, estimated from the Mössbauer spectra of SFA quenched from 1023 K after annealing in air and in H_2–H_2O–N_2 mixture, were verified by the coulometric titration method [17]. The Mössbauer spectroscopy data (table 1) give the total oxygen content of 2.553 and 2.500 per perovskite unit formula for the oxidized and reduced samples, respectively. The values of oxygen content, determined from the coulometric titration data at 1023 K and $p(O_2) = 0.21$ and 10^{-17} atm, are 2.572 and 2.499, correspondingly (figure 3a). The difference between the results of these two techniques is within the limits of experimental uncertainty. Also, charge disproportionation of a few Fe cations in clusters, where

the iron concentration might be locally larger, may lead to a slightly lower Fe^{4+} fraction deduced from the Mössbauer data. Due to the strong overlapping of all contributions to the Mössbauer spectra, absorption due to these Fe cations may have been incorporated in the estimated relative areas of the QS distribution attributed to Fe^{3+} ; the relative areas assigned to Fe^{3+} would thus be slightly overestimated.

In general, the results of the Mössbauer spectroscopy show that reduction of SFA at 1023 K occurs via the formation of brownmillerite-like domains, co-existing with perovskite domains down to relatively low oxygen chemical potentials. Such a behavior is typical for perovskite-like ferrites (see [7,13,20–25] and references cited); analysis of the literature data shows that this local ordering can be expected up to, at least, 1200 K. Furthermore, the catalytic activity of ferrite phases with ordered oxygen sublattice is typically low if compared to disordered perovskites [13]. For the perovskite-related ferrites with ordered microdomains, the maximum catalytic activity is observed at elevated temperatures, 1050–1170 K, when extensive disordering processes start and the perovskite–brownmillerite phase boundary is mobile [11–13]. On the other hand, although one cannot completely exclude the presence of trace amounts of metallic iron on the ferrite surface and its contribution to the catalytic processes [1], the Mössbauer spectroscopy and the data on Pt-modified SFA catalysts both suggest that this effect should be minor. In particular, due to higher catalytic activity and stability of Pt metal with respect to Fe [1], a significantly improved performance could be expected for Pt-modified SFA if the overall process would be governed by metal atoms in the surface monolayer; this is not observed experimentally. Also, the maximum syngas yields are characteristic for partially oxidized ferrite-based catalysts, e.g. when alternate CH_4 and O_2 pulses are supplied over ferrite surface [11,12]. The high catalytic activity of perovskite-related ferrites, such as SFA, towards syngas formation may hence be associated with the lattice instability due to morphotropic phase transformations on reduction.

Acknowledgments

This work was supported by the FCT, Portugal (POCTI program and projects SFRH/BPD/9312/2002, SFRH/BPD/11606/2002 and SFRH/BD/6595/2001) and the NATO Science for Peace program (project 978002). Experimental assistance of Ekaterina Tsipis is gratefully acknowledged.

References

[1] A.P.E. York, T. Xiao and M.L.H. Green, Topics Catal. 22 (2003) 345.
[2] D.J. Wilhelm, D.R. Simbeck, A.D. Karp and R.L. Dickenson, Fuel Process. Technol. 71 (2001) 139.
[3] K. Aasberg-Petersen, J.-H.B. Hansen, T.S. Christensen, I. Dybkjaer, P.S. Christensen, C.S. Nielsen, S.E.L.W. Madsen and J.R. Rostrup-Nielsen, Appl. Catal. A 221 (2001) 379.
[4] T.J. Mazanec, R. Prasad, R. Odegard, C. Steyn and E.T. Robinson, Stud. Surf. Sci. Catal. 136 (2001) 147.
[5] H.J.M. Bouwmeester and A.J. Burggraaf in *Fundamentals of Inorganic Membrane Science and Technology*, A.J. Burggraaf and L. Cot (eds.) (Elsevier, Amsterdam, 1996) pp. 435–528.
[6] M.F. Carolan and P.N. Dyer, US Patent 5569633, (1996).
[7] V.V. Kharton, A.V. Kovalevsky, E.V. Tsipis, A.P. Viskup, E.N. Naumovich, J.R. Jurado and J.R. Frade, J. Solid State Electrochem. 7 (2002) 30.
[8] A.A. Yaremchenko, A.A. Valente, V.V. Kharton, E.V. Tsipis, J.R. Frade, E.N. Naumovich, J. Rocha and F.M.B. Marques, Catal. Lett. 91 (2003) 169.
[9] V.V. Kharton, V.A. Sobyanin, V.D. Belyaev, G.L. Semin, S.A. Veniaminov, E.V. Tsipis, A.A. Yaremchenko, A.A. Valente, I.P. Marozau, J.R. Frade and J. Rocha, Catal. Commun. 5 (2004) 311.
[10] A.L. Shaula, V.V. Kharton, N.P. Vyshatko, E.V. Tsipis, M.V. Patrakeev, F.M.B. Marques and J.R. Frade J. Eur. Ceram. Soc., in press (2004).
[11] F. Martinez-Ortega, C. Batiot-Dupeyrat, G. Valderrama and J.-M. Tatibouët, C.R. Acad. Sci. IIC 4 (2001) 49.
[12] R. Li, C. Yu and S. Shen, J. Nat. Gas Chem. 11 (2002) 137.
[13] V.A. Sadykov, L.A. Isupova, I.S. Yakovleva, G.M. Alikina, A.I. Lukashevich and S. Neophytides, React. Kinet. Catal. Lett. 81 (2004) 393.
[14] L.A. Chick, L.R. Pederson, G.D. Maupin, J.L. Bates, L.E. Thomas and G.L. Exarhos, Mater. Lett. 10 (1990) 6.
[15] J.C. Waerenborgh, M.O. Figueiredo, J.M.P. Cabral and L.C.J. Pereira, Phys. Chem. Min. 21 (1994) 460.
[16] J. Hesse and A. Rübartsch, J. Phys. E 7 (1974) 526.
[17] M.V. Patrakeev, E.B. Mitberg, A.A. Lakhtin, I.A. Leonidov, V.L. Kozhevnikov and K.R. Poeppelmeier, Ionics 4 (1998) 191.
[18] V.V. Kharton, F.M. Figueiredo, A.V. Kovalevsky, A.P. Viskup, E.N. Naumovich, A.A. Yaremchenko, I.A. Bashmakov and F.M.B. Marques, J. Eur. Ceram. Soc. 21 (2001) 2301.
[19] J.R. Frade, V.V. Kharton, A.A. Yaremchenko and E.N. Naumovich, J. Power Sources 130 (2004) 77.
[20] J.P. Hodges, S. Short, J.D. Jorgensen, X. Xiong, B. Dabrowski, S.M. Mini and C.W. Kimball, J. Solid State Chem. 151 (2000) 190.
[21] A. Lebon, P. Adler, C. Bernhard, A.V. Boris, A.V. Pimenov, A. Maljuk, C.T. Lin, C. Ulrich and B. Keimer, Phys. Rev. Lett. 92 (2004) 037202.
[22] J.C. Waerenborgh, F.M. Figueiredo, J.R. Frade, M.T. Colomer and J.R. Jurado, J. Phys. Condens. Mater. 13 (2001) 8171.
[23] C.A. McCammon, A.I. Becerro, F. Langenhorst, R.J. Angel, S. Marion and F. Seifert, J. Phys. Condens. Mater. 12 (2000) 2969.
[24] R.W. Grant, J. Chem. Phys. 51 (1969) 1156.
[25] J.C. Waerenborgh, D.P. Rojas, N.P. Vyshatko, A.L. Shaula, V.V. Kharton, I.P. Marozau and E.N. Naumovich, Mater. Lett. 57 (2003) 4388.